



Removal of lead(II) from aqueous solution using date seed-derived biochar: batch and column studies

Zainab Mahdi¹ · Qiming J. Yu¹ · Ali El Hanandeh¹

Received: 14 May 2017 / Accepted: 18 September 2018 / Published online: 25 September 2018
© The Author(s) 2018

Abstract

This study explored the adsorption of lead ion from aqueous solution onto biochars produced from date seed biomass. Initial evaluation of nine date seed-derived biochars showed that biochar prepared at 550 °C and heating time of 3 h (DSB550-3) was the best adsorbent for Pb²⁺ ion removal. Therefore, it was selected for further investigation in batch and column experiments. The effects of contact time, initial Pb²⁺ concentration, and solution pH were studied. Solution pH showed strong effect on the adsorption ability of DSB550-3 biochar to the lead ion, and the maximum adsorption capacity was found to occur around pH 6.0. The batch maximum adsorption capacity of DSB550-3 biochar was 0.360 mmol g⁻¹. The equilibrium data were adequately fitted to Freundlich and Langmuir isotherms ($R^2=0.97$). The adsorption kinetics were best described by pseudo-second-order model ($R^2=0.94$). The breakthrough curve obtained from the column experiment was best described by the modified dose–response model ($R^2=0.95$). The desorption efficiencies of Pb²⁺ were 2.1%, 23%, 12%, and 55% for DI water, 0.1 M HCl, 0.1 M CaCl₂, and a combination of 0.1 M HCl+0.1 M CaCl₂ eluents, respectively. FTIR analysis and batch experiments results suggested that Pb²⁺ adsorption mechanism was dominated by complexation with active surface groups, precipitation, and cation exchange. Experimental and model results suggested that date seed-derived biochar has high adsorption capacity for Pb²⁺ compared to other plant-based biochars reported in other literature.

Keywords Adsorption · Biochar · Date seed · Desorption · Isotherms · Lead

Introduction

Heavy metals such as lead are highly toxic chemicals that can cause harmful effects to humans and the environment. Lead can enter the ecosystem from natural sources as well as industrial activities such as petroleum refining, electrical and electronic products, and mining. World and Health Organization (WHO) has identified lead as 1 of 10 top toxic pollutants of major public health concern around the world impacting 18–22 million people globally (Liu et al. 2017). Lead can cause severe damage to the nervous system, kidney, brain, and reproductive system (Goel et al. 2005).

Accordingly, the Australian drinking water guidelines set the maximum allowable Pb²⁺ concentration to less than 0.01 mg L⁻¹ (NHMRC 2015).

A variety of physicochemical treatment methods have been developed to control or remove lead from aqueous solutions including ion exchange, chemical precipitation, and membrane separation. Among these methods, adsorption using activated carbon (AC) has been generally recognized as one of the convenient and effective treatment method for Pb²⁺ removal. However, the cost of AC is relatively high. These challenges prompted researchers to investigate more economical, sustainable, and eco-friendly adsorbents to substitute AC for heavy metal removal (El Hanandeh et al. 2016). Biochar application for environmental remediation is an attractive alternative because of the abundance of low-cost biomass that can be used for biochar production. Furthermore, biochar cost is six times cheaper than AC due to the lower energy requirement and the fact that it can be used without further chemical or physical activation (McCarl et al. 2009; Alhashimi and Aktas 2017).

Electronic supplementary material The online version of this article (<https://doi.org/10.1007/s13201-018-0829-0>) contains supplementary material, which is available to authorized users.

✉ Zainab Mahdi
Zainab.mahdi@griffithuni.edu.au

¹ Griffith School of Engineering and Build Environment, Nathan Campus, Griffith University, Nathan, QLD 4111, Australia

Biochar is a carbon-rich material derived from thermal decomposition of organics under oxygen-limited condition. Various precursors have been used for biochar preparation including agricultural waste such as rice husk, pinewood, and sugarcane bagasse (Liu and Zhang 2009; Inyang et al. 2011). Agricultural waste is considered a good source for biochar preparation because they are cheap, safe, renewable, and readily available (Ahmed and Theydan 2012). Although various precursors have been used as potential candidate for biochar preparation, works related to utilization of date seeds as suitable low-cost biochar is limited. Therefore, the present work attempts to assess the adsorption ability of biochar derived from date seed for lead ion removal from aqueous solution.

Date palm tree (*Phoenix Dactylifera L.*) is cultivated in arid and semi-arid regions. It has high tolerance to water shortage and extreme hot temperature. According to the latest statistical data of Food and Agricultural Organization (FAO 2014), the total world production of date was about 8.897 billion tons. Date palm industry is rapidly expanding worldwide, and approximately 35 kg of palm residues per tree is generated annually (Nasser et al. 2016). Date seed biomass is non-edible waste which represents about one-third of the date weight (Sait et al. 2012) making them the largest agricultural by-product in palm-growing countries. Therefore, finding ways to use this agricultural waste sustainably will benefit date producers by creating value-added product as well as offer an environmentally sound waste management option.

Date seed can be introduced as good candidate material to prepare high-quality biochar for heavy metal adsorption from aqueous solution because of its physicochemical properties. Date seed is a carbon-rich material with chemical compositions of lignin, cellulose, hemicellulose, proteins, and hydrocarbons. The lignin contents of the date seed are very high when compared to that of either softwoods or hardwoods (Nasser et al. 2016). Also, the hemicellulose contents of date seed were relatively like those reported by Bledzki et al. (2010) for typical hardwood materials such as coconut shell. The cellulose and hemicellulose have average per cent elemental compositions of 44.4% carbon, 49.4% oxygen, and 6.2% hydrogen (Ahmad et al. 2012). Lignin has a three-dimensional polymer of phenylpropane units linked together by C–O–C or C–C bonds making its elemental composition to be higher in carbon (62%) and lower in oxygen (32%) (Jibril et al. 2008). The high contents of acids of the seeds such as oleic acid are between 41.1 and 58.8% (Al-Shahib and Marshall 2003), which suggests that the seeds are rich with various surface functional groups such as alcohols, phenolic hydroxides, and ethers. Furthermore, date seed is characterized by its low ash content and high volatile matter and therefore, much surface area is generated due to loss of volatile organic matters during pyrolysis

process. Hence, the conversion of date seed into high-quality biochar provides a new solution to the recycle and reuse of non-edible waste to produce valuable products (i.e. biochar) for environmental applications.

Recently, date seed biomass has received considerable attention as a lignin origin for preparing activated carbon (El-Naas et al. 2010). Several studies have examined date seed activated carbon for adsorption purposes (Girgis and El-Hendawy 2002; Bouchelta et al. 2008; Alhamed and Bamufleh 2009; El-Hendawy 2009). Our previous work showed that date seed biochar is characterized by relatively considerable specific surface area, well-developed porous structure, and the presence of various surface functional groups (Mahdi et al. 2016). Furthermore, it showed good adsorption ability for methylene blue (MB) removal from aqueous solution.

Therefore, the present work attempted to assess the adsorption potential of date seed-derived biochar for lead ion removal from aqueous solution. Additionally, most studies encountered in the literature about biochar adsorption were carried out in batch mode which, although provides useful information on adsorption parameters, is not the most practical application in wastewater treatment. Therefore, column experiment was also conducted to provide further information about the adsorption behaviour. The aim of this study was to evaluate the adsorption potential of biochar prepared from date seed under various pyrolysis conditions for Pb^{2+} removal. The equilibrium isotherms, uptake kinetics, column dynamics, and the mechanisms of Pb^{2+} –biochar interaction were investigated in depth.

The objectives of the study were:

- Investigate the Pb^{2+} adsorption capacity of biochar prepared at different pyrolysis conditions.
- Identify optimal biochar preparation conditions to achieve maximize Pb^{2+} adsorption from lead solutions.
- Identify optimal process conditions to maximize adsorption of Pb^{2+} on biochar using batch experiments.
- Investigate the adsorption of Pb^{2+} from aqueous solutions in column experiments.
- Study the leaching potential of Pb^{2+} from loaded biochar.

Materials and methods

Chemicals

All the chemicals used in the experiments were of analytical reagent grade. A 5.0 mM Pb^{2+} stock solution was prepared by dissolving 1.656 g of $Pb(NO_3)_2$ in 1.0 L of deionized water (DI). Then, dilutions of different concentrations ranging from 0.3 to 4.0 mM were prepared. The initial pH of the

solutions was adjusted as needed using 0.1 M NaOH and 0.1 M HCl.

Biochar preparation

Date fruit of full ripeness (Khalas cultivar) was used. The seeds were washed, dried, and then placed in covered crucibles and purged with N₂ gas to provide a low oxygen environment then placed inside a muffle furnace (Lenton furnace). Nine sets of biochars were prepared by varying pyrolysis temperature (350, 450, and 550 °C) and heating time (1, 2, and 3 h). Biochar samples were washed with deionized water to remove fine particles and then crushed and sieved to particle size in the range from 0.6 to 1.4 mm. All the biochars were labelled according to their pyrolysis temperature and heating time (DSBTemp-Time): DSB350-1, DSB350-2, DSB350-3, DSB450-1, DSB450-2, DSB450-3, DSB550-1, DSB550-2, and DSB550-3.

Biochar characterization

Scanning electron microscope (SEM JEOL JSM-6510) was used to examine the surface morphology of biochar before and after Pb²⁺ adsorption. FTIR analysis of the biochar before and after Pb²⁺ adsorption was conducted using (PerkinElmer Spectrum two) to determine the surface functional groups onto the biochar surface. Boehm titration method was used to quantify the acidic functional groups onto biochar surface (Boehm 2002). The pH of biochar was determined according to ASTM D6851 method (ASTM 2011). Biochar specific surface area was determined using methylene blue adsorption (Nunes and Guerreiro 2011). Water-extractable cations and CEC were analysed with a sequential water-BaCl₂ extraction following Kloss et al. (2012) method. Further details on the biomass and biochar physicochemical characteristics are found in our previous work (Mahdi et al. 2016).

Batch adsorption experiments

Screening of different biochars

Biochars prepared at different pyrolysis conditions were screened to compare adsorption uptake capacity of Pb²⁺ from aqueous solution. Biochar (0.10 g) was mixed with 10 mL of Pb²⁺ solution (initial concentration of 0.50 mM) in 50 mL glass container. The initial solution pH was adjusted to 6.0 by adding 0.10 M NaOH or HCl. The mixture was shaken using rotary shaker at 30 rpm for 24 h. Then, the mixture was separated using a 0.45 µm Millex[®] syringe filter. The final concentration of Pb²⁺ was determined using atomic absorption spectroscopy (Avanta-GBC). The amount

of Pb²⁺ adsorbed on the biochar q_e (mmol g⁻¹) is determined by Eq. (1):

$$q_e = \frac{(C_o - C_e)V}{W} \quad (1)$$

where C_o is the initial Pb²⁺ concentration (mM), C_e is the Pb²⁺ concentration at equilibrium (mM), V is the solution volume (L), and W is the biochar dosage (g).

A control run of adsorption experiment was also carried out to investigate the effect of glassware and sampling instruments and showed that the quantity of Pb²⁺ adhering on the container walls and other instruments were negligible (3.65 ± 0.84%). Adsorption performance of date seed biomass in their native form was also investigated and compared to the biochar. All experiments were repeated three times under the same conditions and average values were reported.

Effect of solution pH on adsorption

Solution pH was investigated in the range of 2.0–6.0 by mixing 0.10 g of biochar with 10 mL of Pb²⁺ solution at initial concentration of 0.50 mM in 50 mL glass container. The initial pH of the solution was adjusted using 0.1 M of NaOH or HCl as required. The mixture was shaken using rotary shaker at 30 rpm for 24 h at room temperature (23 ± 2 °C), then the mixture was separated, and the final concentration of Pb²⁺ was determined. Above pH 6.0, precipitations become an issue; therefore, pH values above 6.0 were not studied.

Adsorption isotherms experiments

The Pb²⁺ uptake onto biochar as function of metal concentration was studied by varying Pb²⁺ concentration while keeping all other parameters constant. The experiments were conducted by mixing 0.10 g biochar samples with 10 mL of Pb²⁺ solutions at initial concentrations in the range 0.3–4.0 mM using 50 mL glass container. The experiments were performed at room temperature (23 ± 2 °C) and pH 6.0. The mixture was shaken for 24 h at 30 rpm, and then it was separated using a 0.45 µm Millex[®] syringe filter. The amount of Pb²⁺ adsorbed on the biochar q_e (mmol g⁻¹) is determined using Eq. (1). The relationship between the amounts of metal adsorbed (q_e) and metal concentrations (C_e) at equilibrium was described by Langmuir, Freundlich, and the Temkin isotherms models as shown in Table 1 (see supplementary sheet for further detail).

The thermodynamic equilibrium of Pb²⁺ adsorption was obtained at 25 °C by calculating the Gibbs free energy (ΔG°) for the adsorption process Eq. (2) (Anastopoulos and Kyzas 2016):

$$\Delta G = -RT \ln (K_L \times 55.5 \times 10^3) \quad (2)$$

Table 1 Adsorption equilibrium isotherms

Isotherm	Equation	Description
Langmuir isotherm	$q_e = \frac{q_{\max} K_L C_e}{1 + K_L C_e}$	It proposes a monolayer adsorption onto a surface with a finite number of identical sites
Freundlich isotherm	$q_e = K_F C_e^{\frac{1}{n}}$	It is based on adsorption onto a heterogeneous surface
Temkin isotherm	$q_e = \frac{RT}{b} \ln(AC_e)$	It proposes that the adsorption heat of all the molecules in the layer would decrease linearly with coverage due to adsorbent–adsorbate interactions

where ΔG° is the change in free energy (kJ mol^{-1}), K_L is the equilibrium constant, R is the gas constant ($8.314 \text{ J K}^{-1} \text{ mol}^{-1}$), T is the absolute temperature (K), and $55.5 \text{ (mol L}^{-1})$ is the water concentration.

Adsorption kinetics

The kinetics experiments were performed by mixing 1.0 g of the biochar with 100 mL of Pb^{2+} solution at initial concentration of 0.5 mM, and the solution pH was kept at 6.0. The mixture was shaken for 1440 min using rotary shaker at 30 rpm. Samples were drawn at specified time intervals and analysed. The amount of Pb^{2+} adsorbed at time q_t (mmol g^{-1}) was calculated as:

$$q_t = \frac{(C_o - C_t)V}{W} \quad (3)$$

where C_o is the initial Pb^{2+} concentration (mM), C_t is the Pb^{2+} concentration at given time t (mM), V is the solution volume (L), and W is the biochar weight (g). To explore the adsorption mechanisms of Pb^{2+} uptake onto DSB550-3 biochar, the common kinetic models such as the pseudo-first-order and pseudo-second-order kinetics models were applied to fit the experimental data.

The linearized form of pseudo-first-order model is given as below:

$$\ln(q_e - q_t) = \ln q_e - k_1 t \quad (4)$$

where q_e and q_t are the amount of Pb^{2+} adsorbed (mmol g^{-1}) at equilibrium and at time t , respectively. k_1 (min^{-1}) is the pseudo-first-order adsorption rate constant. The values of k_1 and q_e are obtained from the slopes and intercepts of the linear plot of $\ln(q_e - q_t)$ against t .

A pseudo-second-order kinetic model is expressed in linearized form as in Eq. (5):

$$\frac{t}{q_t} = \frac{1}{k_2 q_e^2} + \frac{t}{q_t} \quad (5)$$

The second-order rate constant k_2 and q_e are obtained from the intercept and the slope of the plot obtained by plotting t/q against time t .

Column adsorption experiments

Column adsorption studies were carried out using glass column of 50 cm length and 2.5 cm internal diameter fitted with a suction filter. To avoid air entrapment, pre-wetted DSB550-3 biochar (bulk density of 490 kg m^{-3}) was packed up with 12 g biochar to the desired bed height (5 cm). The biochar bed was supported by 1 cm layer of glass beads (2.0 mm diameter). Metal solution of 0.5 mM concentration and initial pH of 6.0 was then percolated through the column at a flow rate of 1.0 mL min^{-1} using a peristaltic pump (Masterflex L/S–Cole/Palmer). The effluent samples at the outlet of the column were collected at regular time intervals, and the column was operated until the concentration of metal effluent exceeded 95% of its initial concentration. The experiments were performed in duplicate at room temperature.

The value of the total mass of metal adsorbed, q_t (mmol), can be calculated from the area under the breakthrough curve as shown in Eq. (6):

$$q_t = \frac{Q}{1000} \int_{t=0}^{t=t_b} (C_o - C_t) dt \quad (6)$$

Equilibrium metal uptake or maximum capacity of the column, q_{eq} (mmol g^{-1}), in the column is determined by Eq. (7):

$$q_{\text{eq}} = \frac{q_t}{m} \quad (7)$$

where m is the dry weight of adsorbent in the column (g).

Total amount of metal ion entering column (m_t , mmol) is calculated by Eq. (8):

$$m_t = \frac{C_o Q t_s}{1000} \quad (8)$$

The removal percentage ($R\%$) of lead ions is determined by Eq. (9):

$$R\% = \frac{q_t}{m_t} \times 100 \quad (9)$$

Desorption experiments

Loaded biochar obtained from the earlier experiments were used to determine the desorption behaviour of Pb^{2+} . Deionised water, 0.1 M HCl, 0.1 M $CaCl_2$, and mixture of 0.1 M HCl and 0.1 M $CaCl_2$ were used as desorption agents. The laden biochar was first rinsed with DI water (10 mL) to remove any unabsorbed Pb^{2+} and oven-dried at 50 °C for 24 h. The quantity of Pb^{2+} released into DI water was determined using AAS (Avanta-GBC). Then, dried biochar samples (0.10 g each) were transferred to a clean flask containing 10 mL of 0.1 M HCl, 0.1 $CaCl_2$, or 0.1 M of 50/50 mixture (HCl + $CaCl_2$). The mixture was agitated in rotary shaker at 30 rpm for 24 h. After elution, biochar was filtered to measure the concentration of Pb^{2+} leached in the solution. The desorption efficiency is determined by Eq. (10):

$$\text{Desorption \%} = \frac{\text{amount of metal ion desorbed}}{\text{amount of metal ion adsorbed}} \times 100 \quad (10)$$

Statistical analysis

Regression analysis was used to investigate correlations between pyrolysis conditions and biochar adsorption of Pb^{2+} ion. The analysis was performed using SPSS ver. 22. One-way ANOVA and Tukey post hoc (HSD) tests were also performed to determine the significance of the differences between the adsorption capacities of the biochars prepared at different pyrolysis temperatures and heating time.

Results and discussion

Initial evaluation for Pb^{2+} removal

Figure 1 shows the removal efficiency ($R\%$) of Pb^{2+} ion of the different biochars as a function of pyrolysis temperature and heating time. As shown in Fig. 1, biochar prepared at 550 °C and long heating time 3 h (DSB550-3) showed highest adsorption of Pb^{2+} ion among the tested biochars. The adsorption removal efficiency of Pb^{2+} ion by DSB550-3 was $(96.7\% \pm 0.84\%)$. Furthermore, the lowest removal efficiency $(73.1\% \pm 7.98)$ was observed for DSB350-1 biochar, while the adsorption performance of date seed biomass in their native form had the lowest removal efficiency $(12.8\% \pm 5.51)$.

The removal rate of Pb^{2+} ion increased with the increasing pyrolysis temperature and heating time, which is

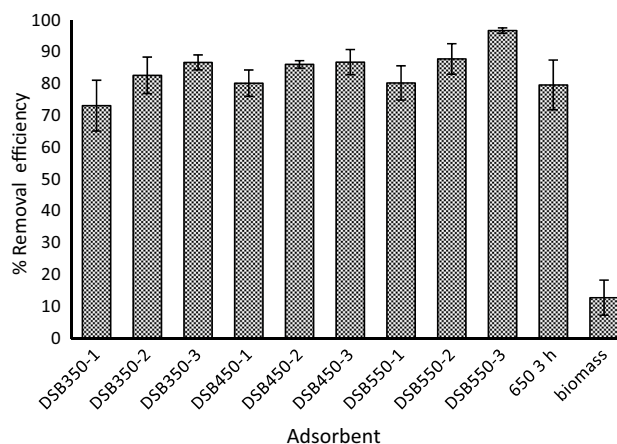


Fig. 1 Adsorption capacity of date seed-derived biochar for Pb^{2+} removal (initial concentration = 0.5 mM; biochar: solution ratio = 10 g L^{-1} ; time = 24 h; pH 6; room temperature; particle size = 0.6–1.4 mm)

consistent with our findings about methylene blue adsorption on date seed biochars (Mahdi et al. 2016). Our results are also in agreement with Yakkala et al. (2013) who investigated Pb^{2+} adsorption using biochar derived from buffalo weed at different pyrolysis temperatures (300, 500 and 700 °C) and reported that adsorption capacity increased with pyrolysis temperature. This can be attributed to the influence of pyrolysis temperature and heating time on the biochar physicochemical characteristics. Regression analysis showed relatively strong correlation between adsorption capacity and the pyrolysis temperature ($r=0.72$) and heating time ($r=0.74$), and these correlations were significant ($p < 0.05$). Furthermore, ANOVA with HSD post hoc analysis revealed that DSB550-3 has significantly higher adsorption capacity for the Pb^{2+} than all other biochars tested in this study. Because DSB550-3 was the best adsorbent, further investigations were conducted to determine the governing adsorption mechanisms of lead ion on the biochar.

Characteristics of biochar

The physicochemical properties of biochar significantly affect its heavy metal adsorption ability and thus the mechanisms governing metal removal by biochar (Li et al. 2017). The physicochemical properties of the biochars prepared in this study are presented in Table 2. The carbon content, ash content, surface area, pH, and CEC of the biochars increased with increasing pyrolytic temperature. The increased percentage of the ash content of biochar (6.79–12.67%) can be attributed to the removal of organic compounds during the pyrolysis. The ash content of biochar samples is positively correlated with biochar pH. Although the pH of biochars varies considerably with pyrolysis temperature, heating

Table 2 Characteristics of biochar prepared at different pyrolysis conditions

Biochar	Surface area (m ² g ⁻¹)	pH	C %	Total acidic groups, mmol			CEC (meq 100 g ⁻¹)
				Carboxyl	Lactone	Phenolic	
DSB350-1	23.88	6.95	64.4	0.47	0.43	0.65	12.47
DSB350-2	69.52	6.99	66.7	0.88	0.30	0.37	14.94
DSB350-3	73.78	7.48	69.0	0.55	0.35	0.50	16.86
DSB450-1	29.86	7.61	63.7	0.55	0.43	0.18	17.02
DSB450-2	97.48	7.69	71.5	0.40	0.78	0.03	20.81
DSB450-3	100.2	7.79	79.3	0.40	0.68	0.03	20.70
DSB550-1	29.56	8.36	69.8	0.50	0.41	0.19	23.69
DSB550-2	88.16	8.43	76.0	0.60	0.20	0.70	21.28
DSB550-3	104.2	8.58	82.2	0.50	0.40	0.30	23.60

time, and type of feedstock (Li et al. 2017), generally, biochar exhibits alkaline nature (Claoston et al. 2014). A positive relationship has been observed between biochar pH and pyrolysis temperature as shown in Table 2. This can be attributed to the release of alkali salts from the organic matrix during the pyrolysis process (Chen et al. 2014; Claoston et al. 2014).

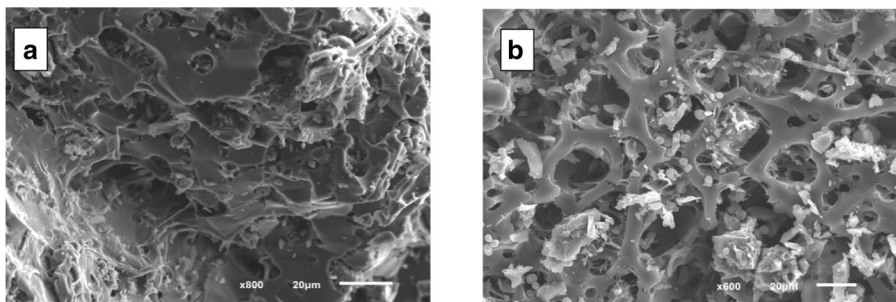
Surface area of biochar is the major physical characteristic that influences adsorption capacity of biochar for heavy metal ions removal (Li et al. 2017). Biochar surface area varies considerably with pyrolysis temperature and heating time. When biomass is subjected to pyrolysis, volatile organic matter is released and progressively increasing surface area of the resultant biochar (Claoston et al. 2014). Increasing the temperature from 500 to 900 °C, Chen et al. (2014) reported that the surface area of biochar increased from 25.4 to 67.6 m² g⁻¹. However, in some cases, biochar produced at high-temperature displays lower surface area due to the destruction or blocking by tar (Li et al. 2017). In our case, biochars prepared at low temperatures and short heating times had smaller surface area which may have limited the Pb²⁺ ions access to the surface-active sites (Table 2).

Biochar mineral composition including potassium (K⁺), calcium (Ca²⁺), magnesium (Mg²⁺), and sodium (Na⁺) can also contribute to metal adsorption via cation exchange capacity (Li et al. 2017). In our study, increasing pyrolysis temperature from 350 to 550 °C led to the increase in total base cations contents in biochar, contributing to increased biochar pH. Furthermore, the disappearance of acidic functional groups such as carboxylic COOH for biochars prepared at higher pyrolysis temperature is another contributor. At higher temperature, biochar yield is lower with high ash content and thus enriching minerals in biochar. The CEC of biochars pyrolyzed at different pyrolysis conditions is given in Table 2, and the results showed that CEC of biochar increased with the increase in pyrolysis temperature. Biochar with high CEC can exhibit higher tendency to adsorb heavy metal cations by releasing light metal cations like K⁺, Ca²⁺, and Mg²⁺ (Wang and Liu 2017).

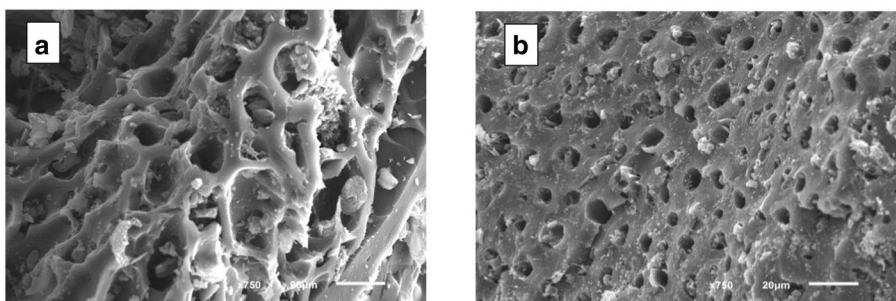
Morphological structure of biochars before and after Pb²⁺ adsorption was examined using SEM spectra as shown in Fig. 2. The SEM images showed that the roughness of the biochar surface and the size of the pores enhanced with increasing pyrolysis temperature. Similar results were also reported by Chen et al. (2017). In general, biomass rich with lignin content develops macroporous biochar, while biomass rich in cellulose yields a predominantly microporous biochar (Joseph et al. 2007). SEM images after Pb²⁺ adsorption further revealed that Pb²⁺ deposition mainly occurred on the biochar surface and in the mesopores rather than micropores. Similar observation was reported by Han et al. (2013) for Cu²⁺ and Zn²⁺ adsorption on switchgrass and woody biochar. This can be due to Pb²⁺ precipitation on the accessible surfaces as well as bonding to active sites (Chen et al. 2011a, b; Kim et al. 2013).

Surface functional groups of biochar such as carboxylic, amino, and hydroxyl groups play important roles in metal adsorption onto biochar. Boehm titration results showed that the total acidic functional groups on biochar surface decreased with increasing pyrolysis temperature from 350 to 550 °C (Table 2). This can be attributed to the higher degree of carbonization suggesting decrease in abundances of hydroxyl (OH) and carboxylic (COOH) groups. This is consistent with the increased biochar pH from 6.95 to 8.58. Similar observation was also reported by Al-Wabel et al. (2013). Surface functional groups of DSB550-3 biochar before and after Pb²⁺ adsorption based on the FTIR spectra were identified as shown in Fig. 3. It can be seen from Fig. 3 that absorption band intensities were shifted after Pb²⁺ adsorption. The shift to higher wave numbers from 1563 to 1678 cm⁻¹ related to the C=O stretching vibration after Pb²⁺ adsorption. This indicates a possible adsorption mechanism involving π - π interactions between Pb²⁺ ion and C=O in carboxylic and ester groups of biochar (Jia et al. 2013). Furthermore, the band peak at approximately 534 cm⁻¹ can be ascribed to the inorganic oxide (Chen et al. 2011b). Therefore, the oxygen-containing functional groups

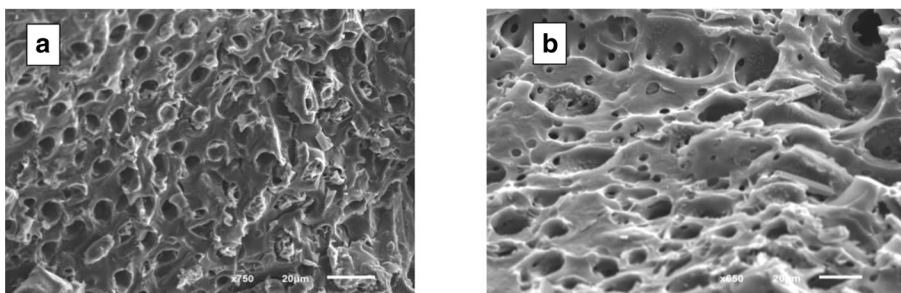
Fig. 2 SEM images for DSB550-3 biochar before and after Pb^{2+} adsorption



DSB550-3 (a) Before Pb^{2+} adsorption, (b) after Pb^{2+} adsorption



DSB450-3 (a) Before Pb^{2+} adsorption, (b) after Pb^{2+} adsorption



DSB550-2 (a) Before Pb^{2+} adsorption, (b) after Pb^{2+} adsorption

onto biochar surface play beneficial role for adsorbing lead ion from aqueous solution.

Based on the above results, the mechanisms controlling Pb^{2+} removal onto date seed-derived biochar can be identified as complexation with surface functional groups, physical adsorption due to porous structure, metal precipitation, and cation exchange mechanism.

Effect of pH on adsorption

The adsorption of Pb^{2+} ion by the DSB550-3 biochar was studied over a pH range of 2–6, keeping all other parameters constant as shown in Fig. 4. It can be seen from Fig. 4, Pb^{2+} adsorption increased linearly from pH 2 to 4, then levelled between pH 4 and 5, before slightly increasing towards pH 6. The maximum Pb^{2+} adsorption was achieved in the pH range between 5 and 6. The maximum “pure” Pb^{2+} adsorption due to pH function may have occurred around pH 5. This range is in agreement with other researchers who reported that the highest adsorption of Pb^{2+} onto date seed activated carbon

was achieved within the pH range 5–6 (Abdulkarim and Abu Al-Rub 2004; Danish et al. 2011). The solution pH affects the surface charge as well as the speciation of the metal ions (Li et al. 2017). At lower pH, competition for binding sites between Pb^{2+} and H^+ results in lower uptake of metal (Bouhamed et al. 2012). The observed increase in adsorption around pH 6 may have been caused by some precipitation as $Pb(OH)_2$ as a result of the solution buffering to pH > 6 during agitation due to the high pH of the biochar. Higher solution pH > 6.0 was avoided due to hydrolyse and precipitation of metal ions as $Pb(OH)_2$. Therefore, all the subsequent experiments in this study were carried out at the optimum initial pH 6.0 to achieve maximum Pb^{2+} removal.

Adsorption kinetics

Figure 5 shows the effect of contact time on Pb^{2+} ion removal. It can be seen from the figure that the adsorption rate reached equilibrium within 360 min and then became practically constant (24 h). This can be explained by the

Fig. 3 FTIR spectra before and after Pb^{2+} adsorption onto the DSB550-3 biochar

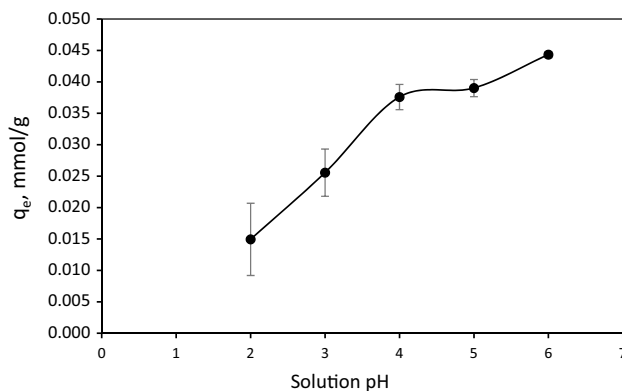
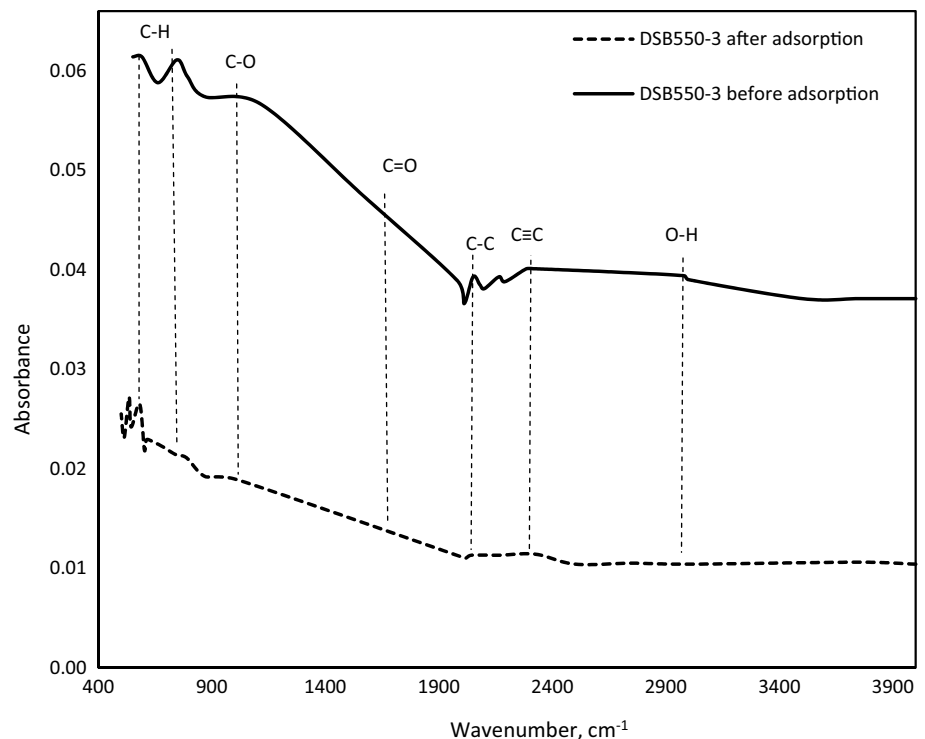


Fig. 4 Effect of solution pH on Pb^{2+} adsorption onto DSB550-3 (initial Pb^{2+} concentration = 0.5 mM; temperature = 23 ± 2 °C; biochar dosage = 10 g L^{-1} ; particle size = 0.60–1.4 mm)

availability and accessibility of vacant adsorption sites on the biochar surface. However, as time passed and active sites were occupied, the remaining vacant sites became difficult to access due to physical constraints and repulsion forces (Cheng et al. 2016).

Adsorption kinetics parameters with the correlation coefficients are represented in Table 3. As shown in Fig. 5, the experimental data are better fitted by pseudo-second-order model ($R^2 = 0.94$) than other kinetics models. This suggests that chemisorption was the dominant mechanism; primarily involved in inner-sphere complexation and precipitation. This agrees with our observations from the FTIR analysis

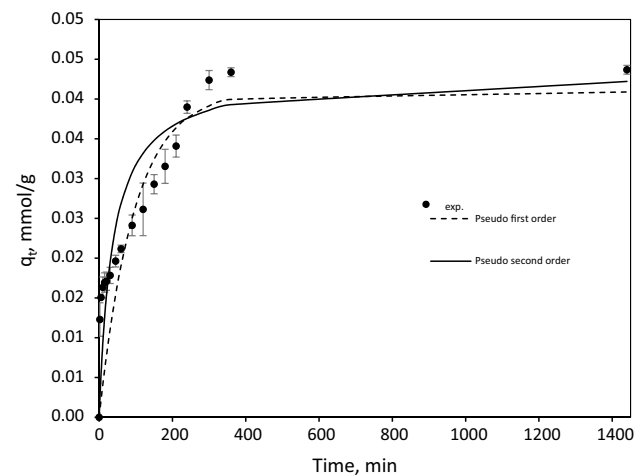


Fig. 5 Effect of contact time on Pb^{2+} adsorption onto DSB550-3 (initial Pb^{2+} concentration = 0.5 mM; pH 6; room temperature; biochar: solution ratio = 10 g L^{-1} ; particle size = 0.6–1.4 mm)

and the SEM images. The relatively long time required to reach equilibrium (360 min) further suggest that electrostatic ion exchange (which commonly reach equilibrium in few minutes) may be comparably small (Zhang and Lo 2006).

Adsorption isotherms

The amount of Pb^{2+} adsorbed onto DSB550-3 biochar increased with increasing initial Pb^{2+} concentrations and

Table 3 Pseudo-first-order and pseudo-second-order kinetic models parameters for Pb²⁺ adsorption on DSB550-3 biochar

Pseudo-first-order model				Pseudo-second-order model			
$k_1 \text{ min}^{-1}$	$q_{\text{exp.}} \text{ (mmol g}^{-1}\text{)}$	$q_{\text{calc.}} \text{ (mmol g}^{-1}\text{)}$	R^2	$k_2 \text{ (g mmol}^{-1} \text{ min}^{-1}\text{)}$	$q_{\text{exp.}} \text{ (mmol g}^{-1}\text{)}$	$q_{\text{calc.}} \text{ (mmol g}^{-1}\text{)}$	R^2
0.011	0.044	0.041	0.86	0.632	0.044	0.042	0.94

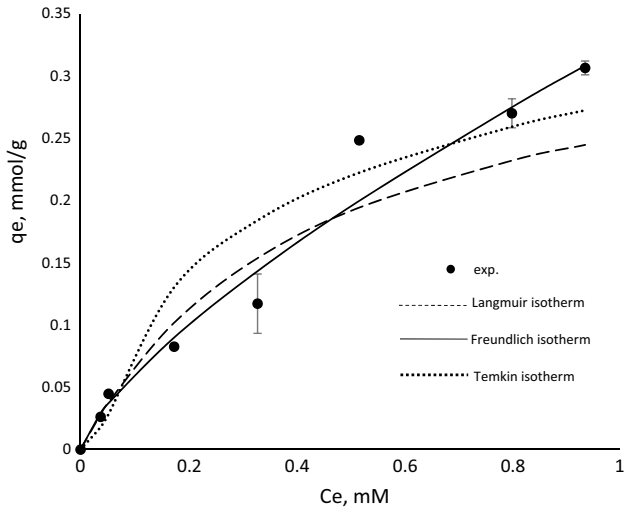


Fig. 6 Equilibrium isotherms of Pb²⁺ adsorption onto DSB550-3 biochar (initial concentration = 0.3–4.0 mM; pH 6; time = 24 h; biochar: solution ratio = 10 g L⁻¹; particle size = 0.6–1.4 mm)

finally reached an upper adsorption limit as shown in Fig. 6. This can be attributed to the limited adsorption sites on biochar surface. At lower Pb²⁺ concentrations, abundant vacant sites were available for Pb²⁺ to be adsorbed on the biochar. However, as Pb²⁺ concentration increased in the solution, the adsorption sites on biochar surface were saturated. As shown in Fig. 6, adsorption isotherm was adequately fitted to both Langmuir and Freundlich equations with a correlation coefficient R^2 of 0.97. Temkin isotherm showed lower fit to the experimental data ($R^2 = 0.88$). Freundlich equation, based on the adsorption intensity value ($n = 1.366$), suggests that the reaction was favourable and that Pb²⁺ adsorption is more of chemisorption than physical adsorption (El Hanandeh et al. 2016). Peruchi et al. (2015) discussed that for $n > 1$, the adsorption occurs on the heterogeneous media where high energy sites were occupied first, followed by adsorption at lower energy sites. Table 4 shows the adsorption isotherms parameters and the correlation coefficients obtained for the linear forms of the isotherms equations.

Table 4 Parameters of adsorption isotherms of Pb²⁺ on DSB550-3 biochar

Langmuir isotherm			Freundlich isotherm			Temkin isotherm		
$K_L \text{ (L mmol}^{-1}\text{)}$	R^2	$q_{\text{max}} \text{ (mmol g}^{-1}\text{)}$	$K_F \text{ [mmol g}^{-1} \text{ (L mmol}^{-1}\text{)}^{1/n}\text{]}$	R^2	$1/n$	$A \text{ (L g}^{-1}\text{)}$	$B \text{ (J mol}^{-1}\text{)}$	R^2
2.271	0.97	0.36	0.324	0.97	0.732	26.95	0.084	0.88

Table 5 Adsorption capacity towards Pb²⁺ from aqueous solution

Adsorbent	Pyrolysis temperature (°C)	pH	$q_{\text{max}} \text{ [mg g}^{-1} \text{ (mmol g}^{-1}\text{)]}$	References
Date seed biochar	550	6.0	74.60 (0.360)	This study
AC from apricot stone	200	6.0	22.85 (0.110)	Kobyas et al. (2005)
Pinewood biochar	300	5.0	4.25 (0.021)	Liu and Zhang (2009)
Rice husk biochar			2.40 (0.012)	
Magnetic pine bark waste char	950	4.0	29.69 (0.143)	Reddy and Lee (2014)
AC from coconut shell	–	4.5	26.50 (0.128)	Sekar et al. (2004)
Date palm fibres	–	4.5	18.62 (0.090)	Al-Haidary et al. (2011)
Date palm leaf and trunk (petiole)			20.04 (0.097)	
Coconut shell AC	–	5.0	21.88 (0.106)	Goel et al. (2005)
Digested sugarcane bagasse biochar	–	–	135.40 (0.653)	Inyang et al. (2011)
Raw sugarcane bagasse biochar			81.90 (0.395)	
Buffalo weed biochar	700	5.0	333.33 (1.608)	Yakkala et al. (2013)

Table 5 shows some of the reported values for lead adsorption on different material. It should be noted that comparison is rather difficult due to the varying experimental conditions employed in these studies such as adsorbent properties, pH, temperature, particle size, and metal concentration. Nevertheless, the data suggest that date seed-derived biochar is a promising adsorption material.

Column adsorption studies

Figure 7 shows the breakthrough curve obtained from the column experiments. The breakthrough time was defined as the point at which the effluent concentration (C_t) reached about 1% of the influent concentration (C_o) and was found to occur at 40 min. The saturation time (t_s) was defined as the point when the effluent concentration reached 99% of C_o and was found to occur at 420 min. As shown in Fig. 7, the breakthrough was reached within the first hour. This might have been caused by the high initial concentration which contributed to the abundance of ions causing saturation of the available sites (Maheshwari and Gupta 2016). The relatively broad transfer zone may be attributed to the slow mass transfer rate which is consistent with the relatively long equilibrium time observed in the uptake kinetic curve (Fig. 5). Insufficient bed depth may have also broadened the mass transfer zone and shortened the breakthrough time (Ahmad and Hameed 2010). Qaiser et al. (2009) found that at lower bed depth, axial dispersion is the governing mechanism of mass transfer. Therefore, insufficient bed depth may lead to short residence time that is insufficient for metal ions to diffuse throughout the bed.

From the breakthrough curve, the total removal ($R\%$) and the equilibrium adsorption capacity (q_{eq} , mmol g^{-1}) were

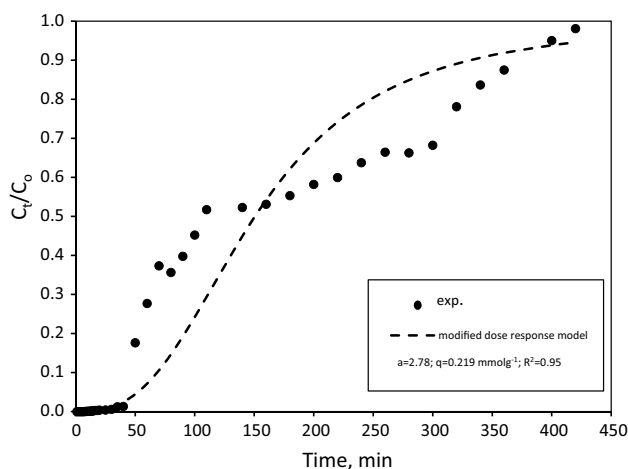


Fig. 7 Breakthrough curve for Pb^{2+} adsorption (bed height=5 cm; flow rate of 1 mL min^{-1} ; initial concentration=0.5 mM; particle size=0.6 mm; pH 6.0)

found to be 43% and 0.007 mmol g^{-1} , respectively. The adsorption capacity for Pb^{2+} uptake onto the biochar was much less than the batch mode results (Fig. 6). Similar observations were reported by Qaiser et al. (2009) and Ahmad and Hameed (2010). This can be attributed to the insufficient contact time (t_b) which did not allow the Pb^{2+} to diffuse into biochar particles and therefore, the adsorption process could be still ongoing and adsorption equilibrium had not been reached. This was consistent with the kinetics results where the required time to reach equilibrium was about 360 min.

Mathematical modelling of fixed bed column adsorption

Several mathematical models have been developed to describe the breakthrough curve for column design including Adams–Bohart, Thomas, and modified dose–response models. Thomas model (Eq. 11) is based on the assumptions of Langmuir’s kinetics of adsorption–desorption and negligible axial and radial dispersion (Malkoc and Nuhoglu 2006):

$$\ln \left(\frac{C_o}{C_t} - 1 \right) = \frac{K_{TH} q_o m}{Q} - K_{TH} C_o t \quad (11)$$

where C_o is influent concentration (mM); C_t is equilibrium concentration (mM) at time t (min); K_{TH} is Thomas constant [$L \text{ min}^{-1} \text{ mmol}^{-1}$]; Q is volumetric flow rate ($L \text{ min}^{-1}$); q_o is the column capacity ($\text{mmol } g^{-1}$) determined by the Thomas model; m is mass of biochar (g). The K_{TH} coefficient and the q_o can be determined from the slope and the intercept of the straight line obtained by plotting $\ln[(C_o/C_t) - 1]$ against t .

Adams–Bohart model (Eq. 12) assumes that equilibrium is not instantaneous and the adsorption rate is proportional to the adsorption capacity remaining on the adsorbent (Goel et al. 2005).

$$t = \frac{N_o Z}{C_o v} - \ln \left(\left(\frac{C_o}{C_t} \right) - 1 \right) \frac{1}{K_{AB} C_o} \quad (12)$$

where t is the breakthrough time (min); C_o the influent concentration (mM); C_t the concentration at breakthrough (mM); N_o the adsorptive capacity ($\text{mmol } L^{-1}$); Z is bed depth (cm); v the linear flow rate ($\text{cm } min^{-1}$); K_{AB} is the Adams–Bohart rate constant [$L (\text{mmol } min)^{-1}$]. Both K_{AB} and N_o can be determined from the slope and the intercept of the straight line obtained by plotting $\ln[(C_o/C_t) - 1]$ against t .

The modified dose–response model (Eq. 13) is a simplified mathematical model which can reduce the error resulting from Thomas model, particularly at lower or higher time periods of the breakthrough curve (Yan et al. 2001).

$$\ln \left[\frac{C_t}{C_o - C_t} \right] = a \ln C_o Q t - a \ln q m \quad (13)$$

where t is the breakthrough time (min); C_0 is influent concentration (mM); C_t is concentration at breakthrough (mM); q the adsorptive capacity (mmol g^{-1}); m biochar weight, (g); a is the modified dose–response model constant. Both a and q can be determined from the slope and the intercept of the straight line obtained by plotting $\ln[C_t/(C_0 - C_t)]$ against $\ln(C_0Qt)$.

Both Adams–Bohart ($R^2 = 0.76$) and Thomas model ($R^2 = 0.77$) showed reasonable fit to the experimental data. However, adsorption experimental data showed better agreement with the modified dose–response model ($R^2 = 0.95$) as shown in Fig. 7. Other researchers also reported that the modified dose–response model can more adequately describe heavy metal adsorption (Yan et al. 2001; Vijayaraghavan and Prabu 2006). According to the modified dose–response model, the maximum Pb^{2+} adsorption capacity (q) in the packed column was found to be $0.219 \text{ mmol g}^{-1}$, which is less than the Langmuir maximum adsorption capacity obtained from the batch experiments ($0.360 \text{ mmol g}^{-1}$). However, Fig. 7 shows that the adsorption of Pb^{2+} onto the biochar displays a two-stage phenomenon which is consistent with our findings from the batch experiment (Fig. 5). The assumed shape of the modified dose–response model does not capture this phenomenon which may have led to inaccurate prediction of the q value.

Adsorption thermodynamics

Adsorption thermodynamic of Pb^{2+} was evaluated by using Gibbs free energy change (ΔG°). The calculated Gibbs free energy value of ($\Delta G^\circ = -29.1$) indicated that the adsorption reaction of Pb^{2+} was a spontaneous process (Anastopoulos and Kyzas 2016).

Desorption studies

Figure 8 shows the results of the desorption experiments. Desorption of Pb^{2+} from the biochar using DI water as eluent agent was negligible ($0.001 \text{ mmol g}^{-1}$, 2.1%) compared to measured amount of adsorbed ($0.046 \text{ mmol g}^{-1}$). HCl was more effective, causing 23% ($0.011 \text{ mmol g}^{-1}$) of the adsorbed lead to desorb. However, a solution composed of 0.01 M HCl and 0.1 M CaCl_2 was the most effective with 55% ($0.026 \text{ mmol g}^{-1}$) desorption efficiency. Biochar has long-term stability in the environment due to its physico-chemical properties and its chemical stability (Harvey et al. 2011; Méndez et al. 2012). Therefore, the results suggest that the loaded biochar may be suitable for disposal into

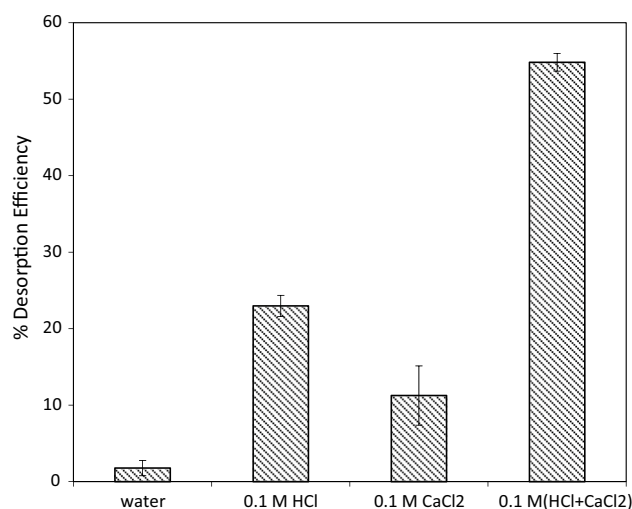


Fig. 8 Desorption studies of laden biochar DSB550-3 with Pb^{2+} ions

designated landfill if it is protected from acidic leachate. Furthermore, if not disposed of in landfill, the exhausted biochar may be regenerated using successive elution with HCl and CaCl_2 .

Conclusions

Lead adsorption on date seed-derived biochar was studied using batch and column experiments. Regression analysis showed that the biochar adsorption capacity for Pb^{2+} was positively and linearly correlated with the pyrolysis temperature and heating time. Biochar prepared at 550°C for 3 h had the highest Pb^{2+} adsorption capacity. The amount of Pb^{2+} adsorbed was found to vary significantly with initial Pb^{2+} concentration, solution pH, and contact time. Langmuir and Freundlich isotherm models were a good fit ($R^2 0.97$) for Pb^{2+} adsorption onto biochar. Maximum adsorption capacity of $0.360 \text{ mmol g}^{-1}$ was obtained at pH of 6.0. Adsorption kinetics showed that the adsorption reaction reached equilibrium after 6 h. Experimental data showed good agreement with the pseudo-second-order kinetic reaction model ($R^2 0.94$). The breakthrough curve obtained from the column study showed good agreement with the predicted results obtained from the modified dose–response model ($R^2 0.95$). The adsorption capacity in the column experiment was found to be $0.219 \text{ mmol g}^{-1}$. The negative adsorption standard free energy changes indicate that the adsorption reaction is spontaneous process. Based on batch and column studies, biochar has the potential to be an efficient sorbent for Pb^{2+} removal from aqueous solution.

Acknowledgements Zainab is a Ph.D. student sponsored by the higher committee for education development in Iraq (HCED). The authors would like to thank Mr. Scott Byrnes, Mr. Alan White, Mr. James Cameron from Griffith University and Ms. Jasmin Rößler from Technische Universität Braunschweig, Germany, for their assistance.

Open Access This article is distributed under the terms of the Creative Commons Attribution 4.0 International License (<http://creativecommons.org/licenses/by/4.0/>), which permits unrestricted use, distribution, and reproduction in any medium, provided you give appropriate credit to the original author(s) and the source, provide a link to the Creative Commons license, and indicate if changes were made.

References

- Abdulkarim M, Abu Al-Rub F (2004) Adsorption of lead ions from aqueous solution onto activated carbon and chemically-modified activated carbon prepared from date pits. *Adsorpt Sci Technol* 22(2):119–134. <https://doi.org/10.1260/026361704323150908>
- Ahmad AA, Hameed BH (2010) Fixed-bed adsorption of reactive azo dye onto granular activated carbon prepared from waste. *J Hazard Mater* 175(1):298–303. <https://doi.org/10.1016/j.jhazmat.2009.10.003>
- Ahmad T, Danish M, Rafatullah M, Ghazali A, Sulaiman O, Hashim R, Ibrahim MNM (2012) The use of date palm as a potential adsorbent for wastewater treatment: a review. *Environ Sci Pollut Res* 19(5):1464–1484. <https://doi.org/10.1007/s11356-011-0709-8>
- Ahmed MJ, Theydan SK (2012) Physical and chemical characteristics of activated carbon prepared by pyrolysis of chemically treated date stones and its ability to adsorb organics. *Powder Technol* 229:237–245. <https://doi.org/10.1016/j.powtec.2012.06.043>
- Al-Haidary AMA, Zanganah FH, Al-Azawi SR, Khalili FI, Al-Dujaili AH (2011) A study on using date palm fibers and leaf base of palm as adsorbents for Pb(II) ions from its aqueous solution. *Water Air Soil Pollut* 214(1–4):73–82. <https://doi.org/10.1007/s11270-010-0405-1>
- Alhamed YA, Bamufleh HS (2009) Sulfur removal from model diesel fuel using granular activated carbon from dates' stones activated by ZnCl₂. *Fuel* 88(1):87–94. <https://doi.org/10.1016/j.fuel.2008.07.019>
- Alhashimi HA, Aktas CB (2017) Life cycle environmental and economic performance of biochar compared with activated carbon: a meta-analysis. *Resour Conserv Recycl* 118:13–26. <https://doi.org/10.1016/j.resconrec.2016.11.016>
- Al-Shahib W, Marshall RJ (2003) The fruit of the date palm: its possible use as the best food for the future? *Int J Food Sci Nutr* 54(4):247–259. <https://doi.org/10.1080/09637480120091982>
- Al-Wabel MI, Al-Omran A, El-Naggar AH, Nadeem M, Usman AR (2013) Pyrolysis temperature induced changes in characteristics and chemical composition of biochar produced from conocarpus wastes. *Biores Technol* 131:374–379. <https://doi.org/10.1016/j.biortech.2012.12.165>
- American Standard Test Method (2011) Standard test method for determination of contact pH with activated carbon (ASTM D6851). <https://doi.org/10.1520/d6851-02r11>
- Anastopoulos I, Kyzas GZ (2016) Are the thermodynamic parameters correctly estimated in liquid-phase adsorption phenomena? *J Mol Liq* 218:174–185. <https://doi.org/10.1016/j.molliq.2016.02.059>
- Australian Government National Health and Medical Research Council (2015) National water quality management strategy (NHMRC): Australian drinking water guideline 6 version 3.1. https://www.nhmrc.gov.au/_files_nhmrc/publications/attachments/eh52_austrian_drinking_water_guidelines_150413.pdf. Accessed 14 Apr 2015
- Bledzki AK, Mamun AA, Volk J (2010) Barley husk and coconut shell reinforced polypropylene composites: the effect of fibre physical, chemical and surface properties. *Compos Sci Technol* 70(5):840–846. <https://doi.org/10.1016/j.compscitech.2010.01.022>
- Boehm HP (2002) Surface oxides on carbon and their analysis: a critical assessment. *Carbon* 40(2):145–149. [https://doi.org/10.1016/s0008-6223\(01\)00165-8](https://doi.org/10.1016/s0008-6223(01)00165-8)
- Bouchelta C, Medjram MS, Bertrand O, Bellat JP (2008) Preparation and characterization of activated carbon from date stones by physical activation with steam. *J Anal Appl Pyrol* 82(1):70–77. <https://doi.org/10.1016/j.jaap.2007.12.009>
- Bouhamed F, Elouear Z, Bouzid J (2012) Adsorptive removal of copper(II) from aqueous solutions on activated carbon prepared from Tunisian date stones: equilibrium, kinetics and thermodynamics. *J Taiwan Inst Chem Eng* 43(5):741–749. <https://doi.org/10.1016/j.jtice.2012.02.011>
- Chen B, Chen Z, Lv S (2011a) A novel magnetic biochar efficiently sorbs organic pollutants and phosphate. *Biores Technol* 102(2):716–723. <https://doi.org/10.1016/j.biortech.2010.08.067>
- Chen X, Chen G, Chen L, Chen Y, Lehmann J, McBride MB, Hay AG (2011b) Adsorption of copper and zinc by biochars produced from pyrolysis of hardwood and corn straw in aqueous solution. *Biores Technol* 102(19):8877–8884. <https://doi.org/10.1016/j.biortech.2011.06.078>
- Chen T, Zhang Y, Wang H, Lu W, Zhou Z, Zhang Y, Ren L (2014) Influence of pyrolysis temperature on characteristics and heavy metal adsorptive performance of biochar derived from municipal sewage sludge. *Biores Technol* 164:47–54. <https://doi.org/10.1016/j.biortech.2014.04.048>
- Chen J, Zhang D, Zhang H, Ghosh S, Pan B (2017) Fast and slow adsorption of carbamazepine on biochar as affected by carbon structure and mineral composition. *Sci Total Environ* 579:598–605. <https://doi.org/10.1016/j.scitotenv.2016.11.052>
- Cheng Q, Huang Q, Khan S, Liu Y, Liao Z, Li G, Ok YS (2016) Adsorption of Cd by peanut husks and peanut husk biochar from aqueous solutions. *Ecol Eng* 87:240–245. <https://doi.org/10.1016/j.ecoleng.2015.11.045>
- Claoston N, Samsuri AW, Ahmad Husni MH, Mohd Amran MS (2014) Effects of pyrolysis temperature on the physicochemical properties of empty fruit bunch and rice husk biochars. *Waste Manage Res* 32(4):331–339. <https://doi.org/10.1177/0734242x14525822>
- Danish M, Hashim R, Rafatullah M, Sulaiman O, Ahmad A (2011) Adsorption of Pb(II) ions from aqueous solutions by date bead carbon activated with ZnCl₂. *Clean Soil Air Water* 39(4):392–399. <https://doi.org/10.1002/clen.201000185>
- El Hanandeh A, Abu-Zurayk RA, Hamadneh I, Al-Dujaili AH (2016) Characterization of biochar prepared from slow pyrolysis of Jordanian olive oil processing solid waste and adsorption efficiency of Hg²⁺ ions in aqueous solutions. *Water Sci Technol* 74(8):1899–1910. <https://doi.org/10.2166/wst.2016.378>
- El-Hendawy ANA (2009) The role of surface chemistry and solution pH on the removal of Pb²⁺ and Cd²⁺ ions via effective adsorbents from low-cost biomass. *J Hazard Mater* 167(1):260–267. <https://doi.org/10.1016/j.jhazmat.2008.12.118>
- El-Naas MH, Al-Zuhair S, Alhajja MA (2010) Reduction of COD in refinery wastewater through adsorption on date-pit activated carbon. *J Hazard Mater* 173(1):750–757. <https://doi.org/10.1016/j.jhazmat.2009.09.002>
- Food and Agriculture Organization of the United Nations FAO (2014) Crop production. USA. <http://www.fao.org/statistics/databases/en/>
- Girgis BS, El-Hendawy ANA (2002) Porosity development in activated carbons obtained from date pits under chemical activation with phosphoric acid. *Microporous Mesoporous Mater* 52(2):105–117. [https://doi.org/10.1016/s1387-1811\(01\)00481-4](https://doi.org/10.1016/s1387-1811(01)00481-4)

- Goel J, Kadirvelu K, Rajagopal C, Garg VK (2005) Removal of lead(II) by adsorption using treated granular activated carbon: batch and column studies. *J Hazard Mater* 125(1):211–220. <https://doi.org/10.1016/j.jhazmat.2005.05.032>
- Han Y, Boateng AA, Qi PX, Lima IM, Chang J (2013) Heavy metal and phenol adsorptive properties of biochars from pyrolyzed switchgrass and woody biomass in correlation with surface properties. *J Environ Manage* 118:196–204. <https://doi.org/10.1016/j.jenvman.2013.01.001>
- Harvey OR, Herbert BE, Rhue RD, Kuo LJ (2011) Metal interactions at the biochar–water interface: energetics and structure–sorption relationships elucidated by flow adsorption microcalorimetry. *Environ Sci Technol* 45(13):5550–5556. <https://doi.org/10.1021/es104401h>
- Inyang M, Gao B, Ding W, Pullammanappallil P, Zimmerman AR, Cao X (2011) Enhanced lead sorption by biochar derived from anaerobically digested sugarcane bagasse. *Sep Sci Technol* 46(12):1950–1956. <https://doi.org/10.1080/01496395.2011.584604>
- Jia M, Wang F, Bian Y, Jin X, Song Y, Kengara FO, Jiang X (2013) Effects of pH and metal ions on oxytetracycline sorption to maize-straw-derived biochar. *Biores Technol* 136:87–93. <https://doi.org/10.1016/j.biortech.2013.02.098>
- Jibril B, Houache O, Al-Maamari R, Al-Rashidi B (2008) Effects of H_3PO_4 and KOH in carbonization of lignocellulosic material. *J Anal Appl Pyrol* 83(2):151–156. <https://doi.org/10.1016/j.jaap.2008.07.003>
- Joseph SD, Downie A, Munroe P, Crosky A, Lehmann J (2007) Biochar for carbon sequestration, reduction of greenhouse gas emissions and enhancement of soil fertility: a review of the materials science. In: Proceedings of the Australian combustion symposium, pp 130–133
- Kim WK, Shim T, Kim YS, Hyun S, Ryu C, Park YK, Jung J (2013) Characterization of cadmium removal from aqueous solution by biochar produced from a giant Miscanthus at different pyrolytic temperatures. *Biores Technol* 138:266–270. <https://doi.org/10.1016/j.biortech.2013.03.186>
- Kloss S, Zehetner F, Dellantonio A, Hamid R, Ottner F, Liedtke V, Soja G (2012) Characterization of slow pyrolysis biochars: effects of feedstocks and pyrolysis temperature on biochar properties. *J Environ Qual* 41(4):990–1000. <https://doi.org/10.2134/jeq2011.0070>
- Kobyas M, Demirbas E, Senturk E, Ince M (2005) Adsorption of heavy metal ions from aqueous solutions by activated carbon prepared from apricot stone. *Biores Technol* 96(13):1518–1521. <https://doi.org/10.1016/j.biortech.2004.12.005>
- Li B, Yang L, Wang CQ, Zhang QP, Liu QC, Li YD, Xiao R (2017) Adsorption of Cd(II) from aqueous solutions by rape straw biochar derived from different modification processes. *Chemosphere* 175:332–340. <https://doi.org/10.1016/j.chemosphere.2017.02.061>
- Liu Z, Zhang FS (2009) Removal of lead from water using biochars prepared from hydrothermal liquefaction of biomass. *J Hazard Mater* 167(1):933–939. <https://doi.org/10.1016/j.jhazmat.2009.01.085>
- Liu W, Tian J, Chen L, Guo Y (2017) Temporal and spatial characteristics of lead emissions from the lead-acid battery manufacturing industry in China. *Environ Pollut* 220:696–703. <https://doi.org/10.1016/j.envpol.2016.10.031>
- Mahdi Z, El Hanandeh A, Yu Q (2016) Influence of pyrolysis conditions on surface characteristics and methylene blue adsorption of biochar derived from date seed biomass. *Waste Biomass Valoriz.* <https://doi.org/10.1007/s12649-016-9714-y>
- Maheshwari U, Gupta S (2016) Removal of Cr(VI) from wastewater using activated neem bark in a fixed-bed column: interference of other ions and kinetic modelling studies. *Desalin Water Treat* 57(18):8514–8525
- Malkoc E, Nuhoglu Y (2006) Removal of Ni(II) ions from aqueous solutions using waste of tea factory: adsorption on a fixed-bed column. *J Hazard Mater* 135(1):328–336. <https://doi.org/10.1016/j.jhazmat.2005.11.070>
- McCarl BA, Peacocke C, Chrisman R, Kung CC, Sands RD (2009) Economics of biochar production, utilization and greenhouse gas offsets. In: Lehmann J, Joseph AS (eds) *Biochar for environmental management: science and technology*. Earthscan, London, pp 341–358
- Méndez A, Gómez A, Paz-Ferreiro J, Gascó G (2012) Effects of sewage sludge biochar on plant metal availability after application to a Mediterranean soil. *Chemosphere* 89(11):1354–1359. <https://doi.org/10.1016/j.chemosphere.2012.05.092>
- Nasser RA, Salem MZ, Hizioglu S, Al-Mefarrej HA, Mohareb AS, Alam M, Aref IM (2016) Chemical analysis of different parts of date palm (*Phoenix dactylifera* L.) using ultimate, proximate and thermo-gravimetric techniques for energy production. *Energies* 9(5):374. <https://doi.org/10.3390/en9050374>
- Nunes CA, Guerreiro MC (2011) Estimation of surface area and pore volume of activated carbons by methylene blue and iodine numbers. *Quim Nova* 34(3):472–476. <https://doi.org/10.1590/s0100-40422011000300020>
- Peruchi LM, Fostier AH, Rath S (2015) Sorption of norfloxacin in soils: analytical method, kinetics and Freundlich isotherms. *Chemosphere* 119:310–317. <https://doi.org/10.1016/j.chemosphere.2014.06.008>
- Qaiser S, Saleemi AR, Umar M (2009) Biosorption of lead from aqueous solution by *Ficus religiosa* leaves: batch and column study. *J Hazard Mater* 166(2):998–1005. <https://doi.org/10.1016/j.jhazmat.2008.12.003>
- Reddy DHK, Lee SM (2014) Magnetic biochar composite: facile synthesis, characterization, and application for heavy metal removal. *Colloids Surf A* 454:96–103. <https://doi.org/10.1016/j.colsurfa.2014.03.105>
- Sait HH, Hussain A, Salema AA, Ani FN (2012) Pyrolysis and combustion kinetics of date palm biomass using thermogravimetric analysis. *Biores Technol* 118:382–389. <https://doi.org/10.1016/j.biortech.2012.04.081>
- Sekar M, Sakthi V, Rengaraj S (2004) Kinetics and equilibrium adsorption study of lead(II) onto activated carbon prepared from coconut shell. *J Colloid Interface Sci* 279(2):307–313. <https://doi.org/10.1016/j.jcis.2004.06.042>
- Vijayaraghavan K, Prabu D (2006) Potential of *Sargassum wightii* biomass for copper(II) removal from aqueous solutions: application of different mathematical models to batch and continuous biosorption data. *J Hazard Mater* 137(1):558–564. <https://doi.org/10.1016/j.jhazmat.2006.02.030>
- Wang Y, Liu R (2017) Comparison of characteristics of twenty-one types of biochar and their ability to remove multi-heavy metals and methylene blue in solution. *Fuel Process Technol* 160:55–63. <https://doi.org/10.1016/j.fuproc.2017.02.019>
- Yakkala K, Yu MR, Roh H, Yang JK, Chang YY (2013) Buffalo weed (*Ambrosia trifida* L. var. *trifida*) biochar for cadmium(II) and lead(II) adsorption in single and mixed system. *Desalin Water Treat* 51(40–42):7732–7745. <https://doi.org/10.1080/19443994.2013.792546>
- Yan G, Viraraghavan T, Chen M (2001) A new model for heavy metal removal in a biosorption column. *Adsorpt Sci Technol* 19(1):25–43. <https://doi.org/10.1260/0263617011493953>
- Zhang W, Lo IM (2006) EDTA-enhanced washing for remediation of Pb- and/or Zn-contaminated soils. *J Environ Eng* 132(10):1282–1288. [https://doi.org/10.1061/\(asce\)0733-9372\(2006\)132:10\(1282\)](https://doi.org/10.1061/(asce)0733-9372(2006)132:10(1282))